



Itinerant electrons, local moments, and magnetic correlations in the pnictide superconductors CeFeAsO_{1-x}F_x and Sr(Fe_{1-x}Co_x)₂As₂

Paolo Vilmercati,¹ Alexei Fedorov,² Federica Bondino,³ Francesco Offi,⁴ Giancarlo Panaccione,⁵ Paolo Lacovig,⁶ Laura Simonelli,⁷ Michael A. McGuire,⁸ Athena S. M. Sefat,⁸ David Mandrus,⁹ Brian C. Sales,⁸ Takeshi Egami,^{1,8,9} Wei Ku,^{10,11} and Norman Mannella^{1,*}

¹*Department of Physics and Astronomy, University of Tennessee, Knoxville, Tennessee 37996, USA*

²*Advanced Light Source, Lawrence Berkeley National Laboratory, Berkeley, California 94720, USA*

³*Laboratorio TASC, IOM-CNR, S.S. 14 km 163.5, Basovizza, I-34149 Trieste, Italy*

⁴*CNISM and Dipartimento di Fisica, Università Roma Tre, via della Vasca Navale 84, I-00146 Rome, Italy*

⁵*Istituto Officina dei Materiali (IOM)-CNR, Laboratorio TASC, Area Science Park, S.S.14, Km 163.5, I-34149 Trieste, Italy*

⁶*Sincrotrone Trieste S.C.p.A., Area Science Park, S.S. 14 km 163.5, I-34149 Trieste, Italy*

⁷*European Synchrotron Radiation Facility, B.P. 220, F-38042 Grenoble, France*

⁸*Materials Science and Technology Division, Oak Ridge National Laboratory, Oak Ridge, Tennessee 37831, USA*

⁹*Department of Materials and Engineering, University of Tennessee, Knoxville, Tennessee 37996, USA*

¹⁰*Condensed Matter Physics and Materials Science Department, Brookhaven National Laboratory, Upton, New York 11973, USA*

¹¹*Physics Department, State University of New York, Stony Brook, New York 11790, USA*

(Received 26 January 2012; revised manuscript received 17 May 2012; published 15 June 2012)

A direct and element-specific measurement of the local Fe spin moment has been provided by analyzing the Fe 3s core level photoemission spectra in the parent and optimally doped CeFeAsO_{1-x}F_x ($x = 0, 0.11$) and Sr(Fe_{1-x}Co_x)₂As₂ ($x = 0, 0.10$) pnictides. The rapid time scales of the photoemission process allowed the detection of large local spin moments fluctuating on a 10^{-15} s time scale in the paramagnetic, antiferromagnetic, and superconducting phases, indicative of the occurrence of ubiquitous strong Hund's magnetic correlations. The magnitude of the spin moment is found to vary significantly among different families, $1.3\mu_B$ in CeFeAsO and $2.1\mu_B$ in SrFe₂As₂. Surprisingly, the spin moment is found to decrease considerably in the optimally doped samples, $0.9\mu_B$ in CeFeAsO_{0.89}F_{0.11} and $1.3\mu_B$ in Sr(Fe_{0.9}Co_{0.1})₂As₂. The strong variation of the spin moment against doping and material type indicates that the spin moments and the motion of itinerant electrons are influenced reciprocally in a self-consistent fashion, reflecting the strong competition between the antiferromagnetic superexchange interaction among the spin moments and the kinetic energy gain of the itinerant electrons in the presence of a strong Hund's coupling. By describing the evolution of the magnetic correlations concomitant with the appearance of superconductivity, these results constitute a fundamental step toward attaining a correct description of the microscopic mechanisms shaping the electronic properties in the pnictides, including magnetism and high-temperature superconductivity.

DOI: [10.1103/PhysRevB.85.220503](https://doi.org/10.1103/PhysRevB.85.220503)

PACS number(s): 74.70.Xa, 74.25.Jb, 74.25.Ha, 79.60.-i

One systematic, key aspect of almost all unconventional superconductivity, as observed in high- T_c cuprates and heavy fermions, is the resilient magnetic correlations in the superconducting state.¹ The same has been observed in the recently discovered iron-based superconductors (Fe-SCs), which offer the possibility for studying the relation between high-temperature superconductivity and magnetic correlations in a wide range of magnetic element-based materials.²

Recent theoretical and experimental results suggest that the nature of the magnetic correlations in Fe-SCs encompasses both the presence of itinerant electrons and local spin moments (LSMs).³⁻¹⁵ While in chalcogenides there is agreement regarding the values of the LSMs measured with different techniques and theoretical calculations, for the pnictides the situation remains puzzling.¹⁶ For the pnictides 122, 111, and 1111 families, agreement regarding the magnitude of the LSM is lacking both between theory and experiments, and among different experiments as well. Specifically, the LSM in the paramagnetic (PM) phase of 122, 111, and 1111 measured with x-ray emission spectroscopy (XES) is found to be $\approx 1\mu_B$, which is consistent with the ordered moments reported in the 122 by other techniques, but larger than

that found in 111 and 1111.¹⁶ Interestingly, while in general density functional theory underestimates the magnitude of the LSM, in the pnictides the opposite happens, with an estimated value $\approx 2\mu_B$.² It has been pointed out how this disagreement originates from the occurrence of fast fluctuations of the LSM whose dynamic develops on time scales of the electron dynamic (10^{-15} s).⁹ The time scale of these fluctuations is shorter than the response time of conventional magnetic probes such as Mössbauer, nuclear magnetic resonance (NMR), and muon spin rotation (μ -SR) spectroscopy, which therefore provide a time-averaged value of the LSM. It is thus very important to carry out measurements with a fast probe in order to determine the true magnitude of the fluctuating LSM.

In this Rapid Communication, we present the measurements of the magnitude of the LSM in 122 and 1111 parent and optimally doped pnictides using core level photoelectron spectroscopy (PES). PES probes the electronic structure on time scales $\approx 10^{-16}$ – 10^{-15} s, much faster than the typical $\approx 10^{-8}$ – 10^{-6} s time scales of Mössbauer, NMR, and μ -SR, and still 1–2 orders of magnitude faster than inelastic neutron scattering (INS). In addition, PES is sensitive to the single-site LSM, as opposed to the correlated moments measured by INS.

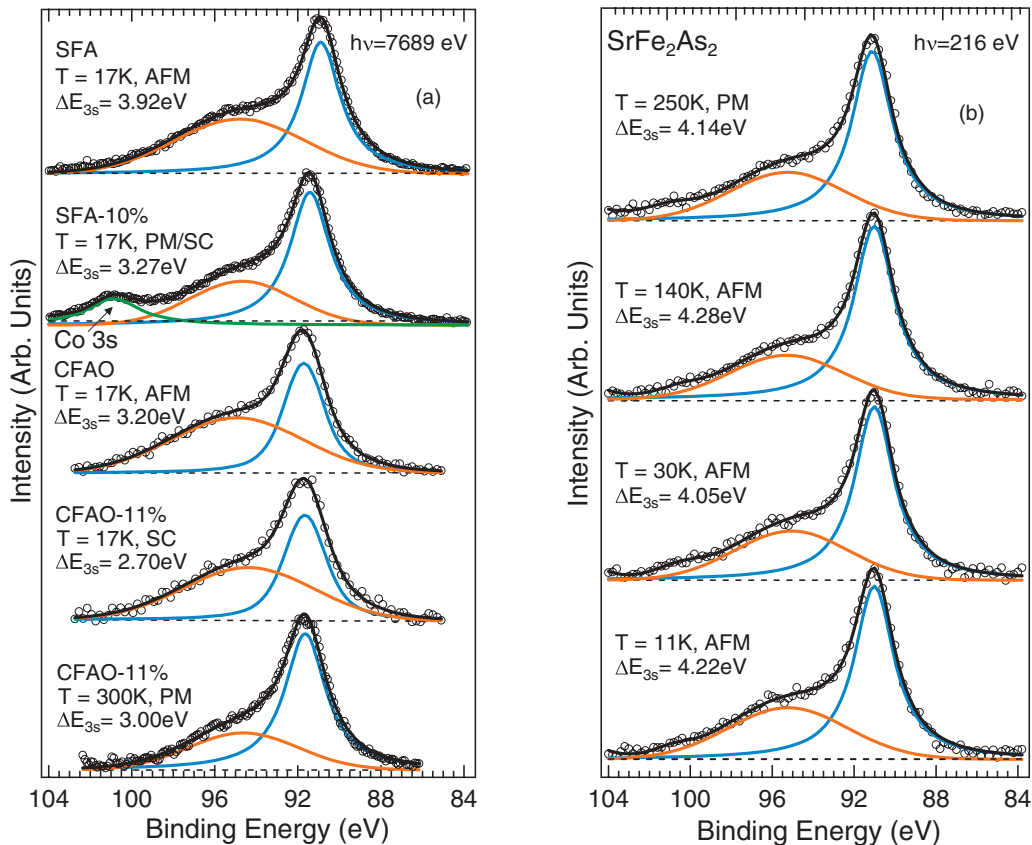


FIG. 1. (Color online) Multiplet splittings in Fe 3s core level HAXPES and PES spectra: Evidence of strong on-site Hund coupling J_H on Fe sites. (a) HAXPES ($h\nu = 7689$ eV) Fe 3s core level spectra in CeFeAsO (CFAO), CeFeAsO_{0.89}F_{0.11} (CFAO-11%), SrFe₂As₂ (SFA), and Sr(Co_{0.12}Fe_{0.88})₂As₂ (SFA-10%) at different temperatures in the antiferromagnetic (AFM), paramagnetic (PM), and superconducting (SC) phases. (b) PES ($h\nu = 216$ eV) Fe 3s core level spectra in SrFe₂As₂ at different temperatures in the PM and AFM phases. A Shirley-type background has been subtracted from the data points (circles). An additional background has been subtracted in the BE region ≈ 105 eV to account for some spectral weight originating from a nearby Auger peak for the spectra excited in SrFe₂As₂ with $h\nu = 216$ eV. The M-SP of the BE is clearly visible as a doublet structure consisting of a main line and a satellite peak at higher BE. The continuous black line through the data points is the result of the two-component fit of the doublet (blue and orange lines beneath). The distance between these two peaks maxima provides the multiplet separation ΔE_{3s} , with experimental uncertainty on ΔE_{3s} of ± 100 meV in (a) and ± 50 meV in (b).

Our data reveal large (i.e., up to $2.1\mu_B$) LSMs fluctuating on $10^{-16} - 10^{-15}$ s time scales in the PM, antiferromagnetic (AFM), and superconducting (SC) phases, indicative of the occurrence of ubiquitous strong Hund's magnetic correlations. While almost insensitive to changes in temperature, the magnitude of the LSM is found to vary against material type and against doping levels. This phenomenology is important for clarifying the relation between high-temperature superconductivity and magnetic correlations.

Polycrystalline CeFeAsO_{1-x}F_x ($x = 0, 0.11$) and Sr(Fe_{1-x}Co_x)₂As₂ ($x = 0, 0.10$) high quality single crystals have been grown and characterized as reported elsewhere.¹⁷⁻¹⁹ Both doped samples are optimally doped with superconducting transition temperatures of 38 K for CeFeAsO_{0.89}F_{0.11} and 14 K for SrFe_{1.8}Co_{0.2}As₂. Bulk-sensitive hard x-ray photoemission (HAXPES) measurements ($h\nu = 7596$ eV) were carried out on beamline ID16 at the ESRF Synchrotron Facility using the Volume Photoemission (VOLPE) spectrometer²⁰ in a pressure lower than 1.5×10^{-9} Torr and total instrumental resolution ≈ 450 meV. Additional low-energy PES measurements ($h\nu = 216$ eV) were carried out on beamline 12.0.1 at

the Advance Light Source with total instrumental resolution ≈ 50 meV. The samples have been measured after being fractured (CeFeAsO_{1-x}F_x) or cleaved [Sr(Fe_{1-x}Co_x)₂As₂] *in situ* at temperatures between 15 and 30 K.

HAXPES and PES Fe 3s core level spectra in different Fe-HTSC compounds are shown in Fig. 1. These spectra exhibit a doublet due to multiplet splitting (M-SP) of the binding energy (BE), a well-known effect in transition metals which provides a unique probe of the LSM of magnetic atoms.²¹⁻²⁵ (See Supplemental Material) The M-SP arises from the exchange coupling of the core 3s electron left behind upon photoelectron emission with the net spin S_V in the unfilled outer shell(s) of the emitter atom (Fe 3d/4s in this case).^{21,22} The Fe 3s doublet originates from the two different BEs of the photoelectrons, depending on whether the spin of the electron left behind is parallel or antiparallel to S_V . The energy difference between the two peaks, referred to as multiplet energy separation ΔE_{3s} , permits estimating the net spin S_V of the emitter atom. To accomplish this, we follow a procedure which has been adopted for itinerant systems, and that has been proven to provide the correct value of S_V , and hence the

LSM.^{26–28} Specifically, work on metallic systems has shown that ΔE_{3s} scales linearly with $(2S_V + 1)$.^{26,27} The values for S_V are obtained by extrapolating the linear fit of the measured splitting ΔE_{3s} plotted against $(2S_V + 1)$ for ionic compounds, for which S_V is known since the valence is an integer number.^{26,27} Multiplying the S_V values by the spin factor $g = 2$, one correspondingly obtains the values for the Fe LSM. We follow this same approach given the itinerant character of the Fe-HTSC.^{26–37} (See Supplemental Material)

The values of ΔE_{3s} are obtained with a two-component fit of the Fe 3s spectra, with uncertainty being estimated to be ± 100 and ± 50 meV for the HAXPES and PES spectra, respectively. The values of ΔE_{3s} , the corresponding S_V values, and the inferred values of the LSM are shown in Fig. 2. The values of the LSM are $1.3\mu_B$ in CeFeAsO and $2.1\mu_B$ in SrFe₂As₂, but decrease to $0.9\mu_B$ and $1.3\mu_B$ in the optimally doped samples, respectively. More specifically, the data show (i) nonvanishing LSMs in all of the phases, (ii) a small temperature dependence of the LSMs, and (iii) a marked dependence of the LSM upon doping. We now comment below on the implication of these observations.

Since M-SP occurs exclusively in atoms with the outer subshell(s) partially occupied with a nonvanishing net spin S_V , the Fe 3s spectra in Fig. 1 indicate that the electronic configuration on the Fe site is never found to be in the “low spin” state $S_V = 0$, indicating that LSMs persist ubiquitously in different phases. A LSM in the PM phase occurs either in the

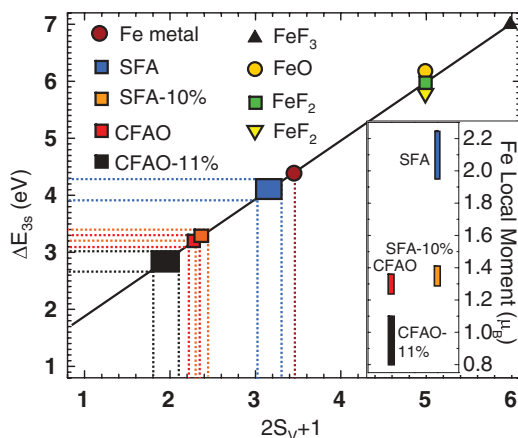


FIG. 2. (Color online) Estimate of the spin moment on the Fe sites from the multiplet energy separation ΔE_{3s} . The data points denote the values of the multiplet energy separation ΔE_{3s} for CeFeAsO (CFAO), CeFeAsO_{0.89}F_{0.11} (CFAO-11%), SrFe₂As₂ (SFA), and Sr(Co_{0.12}Fe_{0.88})₂As₂ (SFA-10%) at different temperatures and phases studied in this work. The continuous line is the extrapolation of the linear fit of the ΔE_{3s} values plotted against $(2S_V + 1)$ for the Fe ionic compounds FeF₃, FeF₂, FeO, for which S_V is known to be $5/2$ (FeF₃) and 2 (FeF₂, FeO) (Ref. 28). The linear fit results in the relation $\Delta E_{3s} = 0.94 + 1.01(2S_V + 1)$. Notably, the value of the SM of metallic Fe is found to be $\approx 2.5\mu_B$, remarkably close to the values of $2.2\mu_B$ and $2.33\mu_B$ measured with neutrons and magnetic susceptibility, giving us confidence in the correctness of this analysis procedure. The size of the symbol is much bigger than the experimental uncertainties: It denotes the range of values for the splitting ΔE_{3s} , the correspondent values for S_V , and the Fe LSM as shown in the inset.

doped samples or above the Néel temperature T_N for the parent compounds, in agreement with previous results.^{16,28} LSMs are also measured in the SC phase of CeFeAsO_{0.89}F_{0.11}, and in proximity to the SC/PM phase boundary in SrFe_{1.8}Co_{0.2}As₂. The presence of a LSM of a similar magnitude has been confirmed further in the SC phase of SrFe_{1.8}Co_{0.2}As₂ with additional data not reported here.

The large values of the Fe LSM indicate the occurrence of a rather strong on-site Hund coupling J_H that fosters the electrons in the Fe 3d/4s shells to align parallel to each other, as suggested by theoretical investigations.^{3,7,8,38} The values for the LSMs shown here are significantly larger than the ordered moments detected in the AFM phase by neutron diffraction, Mössbauer spectroscopy, NMR, and μ -SR.² Most notably, according to our measurements the LSM in SrFe₂As₂ amounts to $2.1\mu_B$, thus indicating a retrieval of the seemingly “missing” LSM in the 122 system.¹⁶ The different time scales involved in the measurements can account for these marked differences.³⁹ Since the photoemission process is fast ($\approx 10^{-16}$ – 10^{-15} s), the values of the LSM extracted from the analysis of the PES Fe 3s spectra are representative of the system sampled over extremely short time scales characteristic of electron dynamics (i.e., a snapshot). In contrast, the time scale of Mössbauer, NMR, and μ -SR measurements are typically $\approx 10^{-8}$ – 10^{-6} s, practically static compared to the time scale of electron dynamics. This discrepancy in the magnitude of the LSM between the fast ($\approx 10^{-16}$ s) and slow (10^{-8} – 10^{-6} s) measurements is due largely to the occurrence of quantum fluctuations, to which only fast measurements are sensitive. Considerations on electron dynamics provide a rationale for the signatures of both itinerant electrons and LSMs exposed by the experiments. In the localized magnetism, as found in insulating transition metal oxides and rare earth metals, LSMs form from well localized electronic wave functions not participating in the Fermi surface (FS). In this case, the magnetism can be discussed by concentrating on the magnetic degrees of freedom alone; it is typically described by spin Hamiltonians, such as the Heisenberg Hamiltonian. This clean separation of magnetic and translational degrees of freedom does not occur in itinerant systems, since the magnetism stems from electrons which also happen to participate in the FS. A unique feature of itinerant systems, with no equivalence in localized magnetism, is that the amplitude of the LSM is not constant, but exhibits very fast fluctuations arising as a result of the electron dynamics. Itinerant electrons have wave functions which are phase coherent over large distances, with the result that the electron density, and as a consequence the spin density, are not described by sharp quantum numbers. If W denotes the bandwidth, itinerant systems are characterized by the presence of a fundamental time scale $\tau_F \approx h/W = \approx 10^{-15}$ s, which is typical of electron motion.⁹ On a time scale $\approx \tau_F$ the magnitude of the LSM is not constant since electrons cannot arrive at and leave a site with sufficient correlation between their spin orientations, thus setting the occurrence of very fast fluctuations in time referred to as *quantum fluctuations*. We stress that the quantum fluctuations are markedly different from spin waves: The latter denote a slower wavelike precession of the atomic moments averaged over the fast quantum fluctuations, with time scales $\tau_{SW} \approx h/W_{SW} \approx 10^{-14}$ – 10^{-13} s, much slower than the fast τ_F .

Quantum fluctuations manifest directly in fast experiments with a short time constant $\approx \tau_F$, and thus involve large energy transfer. This is the case of the Fe 3s spectra in Fig. 1, whose analysis thus provides the values of the bare LSM m_{loc} , which corresponds to the response of the system on short time scales typical of fast quantum fluctuations.⁹ Also the line shape of the Fe 3s spectra is indicative of the occurrence of quantum fluctuations. First, the peak widths are intrinsically large, $\approx 2\text{--}3$ eV, much larger than the experimental resolution. In addition, the best fits to the Fe 3s spectra are always obtained when the curve fitting the peak at higher BE is mainly of Gaussian character, with a width much larger than that of the lower BE peak and larger than that expected from experimental resolution. Indeed, fluctuations in the amplitude of the LSMs on Fe sites should appear in an Fe 3s spectrum as sidebands at higher BE with the peak envelope being a Gaussian, reflecting the normal character of their distribution and the fact that S_V is not a good quantum number.⁴⁰ On the contrary, conventional magnetic experiments average over fast quantum fluctuations since they probe the system on time scales much longer than τ_F , with consequent low-energy transfer. They measure a screened moment which is strongly reduced as compared to the bare LSM m_{loc} .⁹ Although dynamical information can be obtained in INS experiments from integrating the spin susceptibility over energy and momentum,¹⁵ we stress that this analysis provides information about the *correlated* LSM, i.e., $\sum_j \langle S_j S_{i+j} \rangle$, which is a different entity than the bare LSM $\langle S_i \rangle$ measured in PES. The coexistence of local LSMs and itinerant electrons indicates that the physics of Fe-SCs is controlled essentially by different energy scales that correspond to different time limits of the dynamical response of the system: As extremes, one has a large ($\approx \text{eV}$) energy scale, indicative of the quantum fluctuations, and a small ($\approx 1\text{--}100$ meV) energy scale, which corresponds to dressed interactions. The large and small energy scales manifest in the magnetic response of the system as a bare LSM m_{loc} and a screened LSM, respectively.⁹

A significant reduction of the LSM is found by comparing the 122 parent compound with the 1111 parent compound. Even more notably, the reduction of the measured LSM is substantial upon doping in both families. This phenomenology is not compatible with a local-only nature of the LSM, as the local properties of the Fe ion against doping or material type cannot change as much to justify the $\approx 40\%$ reduction of the LSM. On the contrary, these observations reveal the important role played by the itinerant electrons in mediating the magnetism of the pnictides via interaction with the LSM. Interestingly, Hubbard and Hasegawa proposed an amalgam of localized and itinerant models when studying the magnetism in metallic Fe.^{41–43} They pointed out that the motion of the itinerant electrons and the configurations of the exchange fields, entities essentially proportional to the local LSMs of atoms, are influenced reciprocally in a self-consistent fashion.^{41–43} In a context specific to the pnictides, it has been discussed how the interaction between the LSMs is mediated by the itinerant electrons in a self-consistent fashion thanks to the provision of additional degrees of freedom such as the low electron kinetic energy and a twofold orbital freedom, i.e., the degeneracy of the d_{xz} and d_{yz} orbitals.^{7,8,44,45} The large contribution of the itinerant electrons in increasing the kinetic energy gain and the

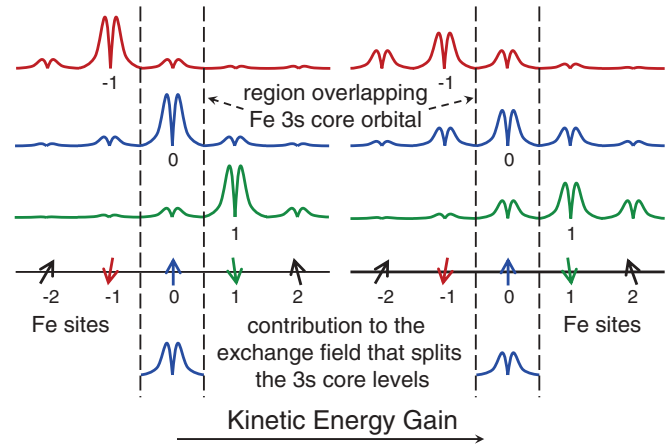


FIG. 3. (Color online) Reduction of the local moment upon enhanced kinetic energy gain. Schematic of spatial distribution of the fluctuating spins centered at Fe sites (labeled by integer numbers), upon “integrating out” the higher-energy degrees of freedom that correspond to fluctuations faster than the PES time scale ($\approx 10^{-16}$ s). More precisely, the schematic illustrates the spin-polarized Wannier orbitals that span the remaining low-energy fermionic space. With enhanced effective kinetic processes (upon doping away from an integer number of electrons per Fe, applying pressure, or changing the Fe-As-Fe bond angle), the spatial extent of the fluctuating spin increases, as shown in the right panel, and consequently the central contribution decreases. In turn, the exchange field applied to the region spanned by the 3s core orbital (within dashed lines) reduces, producing a smaller multiplet splitting in the 3s PES. Such a high-energy kinetic driven reduction is most visible in the presence of strong short-range AFM correlations, in which case the tails from neighboring spins gives opposite contributions.

twofold orbital degeneracy provide degrees of freedom which add significant flexibility to how the itinerant electrons can interact with different local magnetic correlations.

The reduction of the measured LSM against doping and material type can be rationalized as a consequence of increasing the kinetic energy gain, achieved by spreading out the spatial distribution of the fluctuating spins (spin-polarized Wannier orbitals) onto multiple atomic sites (cf. Fig. 3). As a consequence, the exchange field at a particular site in the region spanned by the 3s core orbital is reduced, which in turn is responsible for the systematic reduction of ΔE_{3s} in the Fe 3s core level spectra, and hence the measured LSM. An additional effect responsible for the reduction of the exchange field at a particular site is the strong short-range AFM correlations, in which case the tails from neighboring spins give opposite contributions (cf. Fig. 3). The reduction associated with the large values of the LSMs exposed by our data reflect the strong competition between the AFM superexchange interaction among the LSMs, and the kinetic energy gain of the itinerant electrons in the presence of a strong Hund’s coupling.^{7,8} Note that since the LSMs fluctuate at a high frequency, the reported large LSMs have irrelevant effects on the low-energy pair-breaking processes.

In conclusion, we presented experimental evidence of large (up to $2.1\mu_B$) LSMs fluctuating on quantum time scales in the PM, AFM, and SC phase of pnictides using core level PES, an experiment sensitive to the single-site moment that probes

the electronic structure on a much faster time scale than that of conventional magnetic probes. The data reveal a large LSM fluctuating on a 10^{-15} s time scale amounting to $2.1\mu_B$ in SrFe_2As_2 and $1.3\mu_B$ in CeFeAsO , which decreases to $1.35\mu_B$ and $0.9\mu_B$ in the optimally doped samples. The very large size of the LSM is evidence for the occurrence of strong Hund's magnetic correlations. The strong variation of the LSM against doping and material type indicates that the LSM and the motion of itinerant electrons are influenced reciprocally in a self-consistent fashion, reflecting the strong competition between the AFM superexchange interaction among the LSMs, and the kinetic energy gain of the itinerant electrons in the presence of a strong Hund's coupling. Our study encourages

development of future understandings of magnetism and superconductivity along similar lines of consideration, namely, correlated metals under the influence of strong coupling to LSMs.

The work at ALS and European Synchrotron Radiation Facility is supported by NSF Grant No. DMR-0804902. The work at Oak Ridge is sponsored by the Division of Materials Science and Engineering, Office of Basic Energy Sciences. Oak Ridge National Laboratory is managed by UT-Battelle, LLC, for the US Department of Energy under Contract No. DE-AC05-00OR22725. Financial support by Eugene P. Wigner Fellows at ORNL is acknowledged.

*nmannell@utk.edu

- ¹S. Li and P. Dai, *Front. Phys.* **6**, 429 (2011).
- ²D. C. Johnston, *Adv. Phys.* **59**, 803 (2010).
- ³M. D. Johannes and I. I. Mazin, *Phys. Rev. B* **79**, 220510 (2009).
- ⁴Y.-Z. You, F. Yang, S.-P. Kou, and Z.-Y. Weng, *Phys. Rev. B* **84**, 054527 (2011).
- ⁵S.-P. Kou, T. Li, and Z.-Y. Weng, *Europhys. Lett.* **88**, 17010 (2009).
- ⁶L. de Medici, S. R. Hassan, and M. Capone, *J. Supercond. Novel Magn.* **22**, 533 (2009).
- ⁷W.-G. Yin, C.-C. Lee, and W. Ku, *Phys. Rev. Lett.* **105**, 107004 (2010).
- ⁸W. Lv, F. Krüger, and P. Phillips, *Phys. Rev. B* **82**, 045125 (2010).
- ⁹P. Hansmann, R. Arita, A. Toschi, S. Sakai, G. Sangiovanni, and K. Held, *Phys. Rev. Lett.* **104**, 197002 (2010).
- ¹⁰J. Zhao, D. T. Adroja, D.-X. Yao, R. Bewley, S. Li, X. F. Wang, G. Wu, X. H. Chen, J. Hu, and P. Dai, *Nat. Phys.* **5**, 555 (2009).
- ¹¹S. O. Diallo, V. P. Antropov, T. G. Perring, C. Broholm, J. J. Pulikotil, N. Ni, S. L. Bud'ko, P. C. Canfield, A. Kreyssig, A. I. Goldman, and R. J. McQueeney, *Phys. Rev. Lett.* **102**, 187206 (2009).
- ¹²S. J. Moon, J. H. Shin, D. Parker, W. S. Choi, I. I. Mazin, Y. S. Lee, J. Y. Kim, N. H. Sung, B. K. Cho, S. H. Khim, J. S. Kim, K. H. Kim, and T. W. Noh, *Phys. Rev. B* **81**, 205114 (2010).
- ¹³N. L. Wang, W. Z. Hu, Z. G. Chen, R. H. Yuan, G. Li, G. F. Chen, and T. Xiang, *arXiv:1105.3939*.
- ¹⁴A. A. Schafgans, S. J. Moon, B. C. Pursley, A. D. LaForge, M. M. Qazilbash, A. S. Sefat, D. Mandrus, K. Haule, G. Kotliar, and D. N. Basov, *Phys. Rev. Lett.* **108**, 147002 (2012).
- ¹⁵M. Liu, L. W. Harriger, H. Luo, M. Wang, R. A. Ewings, T. Guidi, H. Park, K. Haule, G. Kotliar, S. M. Hayden, and P. Dai, *Nat. Phys.* **8**, 376 (2012).
- ¹⁶H. Gretarsson, A. Lupascu, J. Kim, D. Casa, T. Gog, W. Wu, S. R. Julian, Z. J. Xu, J. S. Wen, G. D. Gu, R. H. Yuan, Z. G. Chen, N.-L. Wang, S. Khim, K. H. Kim, M. Ishikado, I. Jarrige, S. Shamoto, J.-H. Chu, I. R. Fisher, and Y.-J. Kim, *Phys. Rev. B* **84**, 100509(R) (2011).
- ¹⁷A. S. Sefat, M. A. McGuire, B. C. Sales, R. Jin, J. Y. Howe, and D. Mandrus, *Phys. Rev. B* **77**, 174503 (2008).
- ¹⁸M. A. McGuire, R. P. Hermann, A. S. Sefat, B. C. Sales, R. Jin, D. Mandrus, F. Grandjean, and G. J. Long, *New J. Phys.* **11**, 025011 (2009).
- ¹⁹A. S. Sefat, R. Jin, M. A. McGuire, B. C. Sales, D. J. Singh, and D. Mandrus, *Phys. Rev. Lett.* **101**, 117004 (2008).
- ²⁰P. Torelli, M. Sacchi, G. Cautero, M. Cautero, B. Krastanov, P. Lacovig, P. Pittana, R. Sergo, R. Tommasini, A. Fondacaro, F. Offi, G. Paolicelli, G. Stefani, M. Gironi, R. Verbeni, G. Monaco, and G. Panaccione, *Rev. Sci. Instrum.* **76**, 023909 (2005).
- ²¹C. S. Fadley, D. A. Shirley, A. J. Freeman, P. S. Bagus, and J. V. Mallow, *Phys. Rev. Lett.* **23**, 1397 (1969).
- ²²C. S. Fadley, *Electron Spectroscopy, Theory, Techniques, and Applications* (Pergamon, Oxford, 1978), Vol. II, Chap. 1.
- ²³G.-H. Gweon, J.-G. Park, and S.-J. Oh, *Phys. Rev. B* **48**, 7825 (1993).
- ²⁴L. Sangaletti, L. E. Depero, P. S. Bagus, and F. Parmigiani, *Chem. Phys. Lett.* **245**, 463 (1995).
- ²⁵F. Parmigiani and L. Sangaletti, *J. Electron. Spectrosc. Relat. Phenom.* **98–99**, 287 (1999).
- ²⁶F. R. McFeely, S. P. Kowalczyk, L. Leyt, and D. A. Shirley, *Solid State Commun.* **15**, 1051 (1974).
- ²⁷D. G. Van Campen and L. E. Klebanoff, *Phys. Rev. B* **49**, 2040 (1994).
- ²⁸F. Bondino, E. Magnano, M. Malvestuto, F. Parmigiani, M. A. McGuire, A. S. Sefat, B. C. Sales, R. Jin, D. Mandrus, E. W. Plummer, D. J. Singh, and N. Mannella, *Phys. Rev. Lett.* **101**, 267001 (2008).
- ²⁹F. U. Hillebrecht, R. Jungblut, and E. Kisker, *Phys. Rev. Lett.* **65**, 2450 (1990).
- ³⁰J. F. van Acker, Z. M. Stadnik, J. C. Fuggle, H. J. W. M. Hoekstra, K. H. J. Buschow, and G. Stroink, *Phys. Rev. B* **37**, 6827 (1988).
- ³¹B. D. Hermsmeier, C. S. Fadley, B. Sinkovic, M. O. Krause, J. Jimenez-Mier, P. Gerard, T. A. Carlson, S. T. Manson, and S. K. Bhattacharya, *Phys. Rev. B* **48**, 12425 (1993).
- ³²H. Capellman, *J. Magn. Magn. Mater.* **28**, 250 (1982).
- ³³B. L. Gyorffyt, A. J. Pindors, J. Staunton, G. M. Stocks, and H. A. Winter, *J. Phys. F* **15**, 1337 (1985).
- ³⁴A. Subedi and D. J. Singh, *Phys. Rev. B* **81**, 024422 (2010).
- ³⁵B. P. Neal, E. R. Ylvisaker, and W. E. Pickett, *Phys. Rev. B* **84**, 085133 (2011).
- ³⁶M. Oku, N. Masahashi, S. Hanada, and K. Wagatsuma, *J. Alloys Compd.* **413**, 239 (2006).
- ³⁷A. G. Petukhov, I. I. Mazin, L. Chioncel, and A. I. Lichtenstein, *Phys. Rev. B* **67**, 153106 (2003), and references therein.

³⁸K. Haule and G. Kotliar, *New J. Phys.* **11**, 025021 (2009).

³⁹See Supplemental Material at <http://link.aps.org/supplemental/10.1103/PhysRevB.85.220503> for a comparison of our findings with the results of XES measurements reported in Ref. 16.

⁴⁰We stress that when materials are nonmagnetic with an almost temperature-independent magnetic susceptibility (e.g., Rh metal), no exchange splitting is measured in the $3s$ spectrum. This is different from spin fluctuations in the paramagnetic phase of ionic

systems. In this case, with the fast PES probe, all Fe atoms would exhibit the same large moment.

⁴¹J. Hubbard, *Phys. Rev. B* **19**, 2626 (1979).

⁴²J. Hubbard, *Phys. Rev. B* **20**, 4584 (1979).

⁴³H. Hasegawa, *J. Phys. Soc. Jpn.* **46**, 1504 (1979).

⁴⁴W. Lv, J. Wu, and P. Phillips, *Phys. Rev. B* **80**, 224506 (2009).

⁴⁵C.-C. Lee, W.-G. Yin, and W. Ku, *Phys. Rev. Lett.* **103**, 267001 (2009).